Modeling, Computer Aided Design, and Construction of a Furuta Pendulum Test-Bed

Mayra Antonio-Cruz[1], Ramón Silva-Ortigoza[1],
Carlos Alejandro Merlo-Zapata[1], Victor Manuel Hernández-Guzmán[2],
Celso Márquez-Sánchez[1], and Jacobo Sandoval-Gutiérrez[1]

[1] Instituto Politécnico Nacional, CIDETEC, Área de Mecatrónica.
Unidad Profesional Adolfo López Mateos, CP. 07700, México, DF, Mexico.

[2] Universidad Autónoma de Querétaro, Facultad de Ingeniería.
CP. 76150, Querétaro, Qro., Mexico.

Abstract. This paper presents a Furuta pendulum as a test-bed to experimentally validate automatic control strategies or theoretical concepts associated with nonlinear systems. Herein, the modeling, computer aided design, and construction of a Furuta pendulum test-bed is introduced step-by-step. The deduction of the Furuta pendulum mathematical model is achieved by using Lagrange equations of motion. In contrast with other works, this model deduction includes an analysis of the system kinematics. Furthermore, a computer aided design of the Furuta pendulum is carried out via the software SolidWorks, based on such a design a test-bed is built. Numerical simulations of the Furuta pendulum model are performed via Matlab-Simulink. Moreover, with the intention of verifying that the test-bed built behaves according to the model herein deduced, experimental tests with the test-bed in open-loop are carried out by using Matlab-Simulink, ControlDesk, and a DS1104 board from dSPACE.

Keywords: Underactuated system; Furuta Pendulum; Test-Bed; Modeling; Computer Aided Design; Construction.

1 Introduction

In last decades, control engineering researchers have had a strong interest on the underactuated mechanical systems. This interest is due to such systems exhibit various problems that can be observed in industrial applications, such as external disturbances and nonlinear behaviors under different operation conditions [1]. Particularly, the Furuta Pendulum –also known as rotary inverted pendulum– is a mechanism that has two degrees of freedom (DOF) and two rotational joints. It is essentially integrated of three elements: a motor and two bars called *arm* and *pendulum*. The motor's shaft is connected to one end of the *arm*, which causes the *arm* to be moved angularly in the horizontal plane, whereas the *pendulum* is joined to the free end of the *arm* through a link that can move freely and allows

Advances in Computer Science
Research in computing Science 83, 2014 pp. 133-144

the rotation of the *pendulum* in the vertical plane. This mechanism is a popular device that has been used both as benchmark for the analysis of nonlinear control and for educational purposes (see, for example [2–8]).

Literature associated with the modeling and construction of the Furuta pendulum is as follows. Regarding the modeling, Acosta [9] described a quasi-conservative dynamic model, derived from the classical mechanics, which allows designing all the controllers as if the system was conservative. Another work provided by Cazzolato and Prime [10], introduces a dynamics of the Furuta pendulum considering a full inertia tensor. That dynamics was derived by using two methods: a Lagrangian formulation and an iterative Newton-Euler formulation. Jadlovská and Sarnovský [1] presented an application of a general procedure to derive a mathematical model of the rotary inverted pendulum with an arbitrary number of pendulum links. To design such a model Lagrangian equations and a Rayleigh dissipation function were used. The validity of the mathematical model generated by the application were shown via numerical simulations. As regards the construction, Allotta *et al.* [11] constructed two different prototypes of the Furuta pendulum with the intention of providing test-beds for the laboratories of mechatronics and complex dynamics, and systems control of the University of Florence. In addition, the dynamic parameter identification of the real prototype was carried out. In the study of García-Alarcón *et al.* [12], a procedure to achieve the parameter identification of an experimental system associated with the Furuta pendulum, a computer aided design and the system built were shown. Also, in order to validate such a procedure, results from numerical simulations of the system dynamic model were compared with experimental results from the system built. On the other hand, a work that describes step-by-step both the modeling and construction of a Furuta pendulum prototype was introduced recently by Antonio-Cruz *et al.* [13]. In that work numerical simulations of the Furuta pendulum mathematical model were performed. Likewise, the prototype built was experimentally tested to show its real behavior.

Having undertaken the literature review, it was found that few works have been exclusively dedicated to the modeling, computer aided design, and construction of a Furuta pendulum. Also, in such works, the Furuta pendulum mathematical model is not described step-by-step and most of them do not include the kinematic analysis of the system. Furthermore, to the authors' knowledge, papers where the computer aided design along with the construction of a Furuta pendulum test-bed are described step-by-step have not been reported until now. The aforementioned could be of great help, since to implement or validate automatic control strategies in real time, the modeling, computer aided design, and construction of a Furuta pendulum test-bed are required. Thus, in order to contribute in this direction, this paper presents the modeling, computer aided design, and construction step-by-step of a Furuta pendulum test-bed, including the corresponding experimental verification.

The remaining of the paper is structured as follows. Section 2 deals with the deduction of the Furuta pendulum mathematical model; whereas, the design and construction of the system under study is treated in Section 3. The numerical simulations of the Furuta pendulum model and the experimental tests of the test-bed built are shown in Section 4. Lastly, the conclusion is given in Section 5.

2 Modeling

A graphical representation of the Furuta pendulum is shown in Figure 1. There, θ_0 is the *arm* angular position measured with respect to an arbitrary position, θ_1 is the *pendulum* angular position measured with respect to the upright position, τ is the torque (applied to the *arm*) generated by the electric motor, I_0 is the *arm* inertia (when it turns around one of its ends) and the motor inertia, L_0 is the *arm* length, m_1, l_1, and J_1 are the mass, the center of mass location, and the *pendulum* inertia, respectively. Lastly, $g = 9.81$ m/s^2 represents the gravity acceleration.

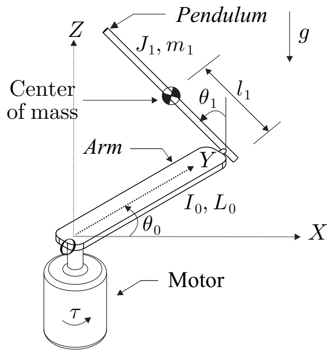

Fig. 1. Furuta pendulum.

As the Furuta pendulum is a two DOF system, its dynamic model is given by two Lagrange equations of motion, which are defined by

$$\frac{d}{dt}\left(\frac{\partial L}{\partial \dot{\theta}_0}\right) - \frac{\partial L}{\partial \theta_0} = \tau, \tag{1}$$

$$\frac{d}{dt}\left(\frac{\partial L}{\partial \dot{\theta}_1}\right) - \frac{\partial L}{\partial \theta_1} = 0, \tag{2}$$

where $\dot{\theta}_0$ is the *arm* angular velocity, $\dot{\theta}_1$ the *pendulum* angular velocity, and L the system Lagrangian determined as

$$L = K - V, \tag{3}$$

being K and V the kinetic energy and potential energy, respectively, of the Furuta pendulum system.

On the one hand, K is the sum of the kinetic energy of the *arm* and the *pendulum*, which are, respectively, defined as follows:

$$K_0 = \frac{1}{2} I_0 \dot{\theta}_0^2, \tag{4}$$

$$K_1 = \frac{1}{2} J_1 \dot{\theta}_1^2 + \frac{1}{2} m_1 \upsilon_1^T \upsilon_1, \tag{5}$$

where υ_1 is the linear velocity of the *pendulum* center of mass. Hence, an analysis of the Furuta pendulum kinematics is required. Then, from Figure 2, the location of the *pendulum* center of mass is determined by

$$x = [x_x,\ x_y,\ x_z]^T, \tag{6}$$

where x_x, x_y, and x_z are defined as follows:

$$x_x = L_0 cos(\theta_0) - l_1 sin(\theta_1) sin(\theta_0), \qquad x_y = L_0 sin(\theta_0) + l_1 sin(\theta_1) cos(\theta_0),$$
$$x_z = l_1 cos(\theta_1).$$

Thus, υ_1 is given by

$$\upsilon_1 = [\dot{x}_x,\ \dot{x}_y,\ \dot{x}_z]^T, \tag{7}$$

being

$$\dot{x}_x = -\dot{\theta}_0 L_0 sin(\theta_0) - l_1 \left(\dot{\theta}_0 sin(\theta_1) cos(\theta_0) + \dot{\theta}_1 sin(\theta_0) cos(\theta_1)\right),$$
$$\dot{x}_y = \dot{\theta}_0 L_0 cos(\theta_0) + l_1 \left(\dot{\theta}_1 cos(\theta_0) cos(\theta_1) - \dot{\theta}_0 sin(\theta_0) sin(\theta_1)\right),$$
$$\dot{x}_z = -\dot{\theta}_1 l_1 sin(\theta_1).$$

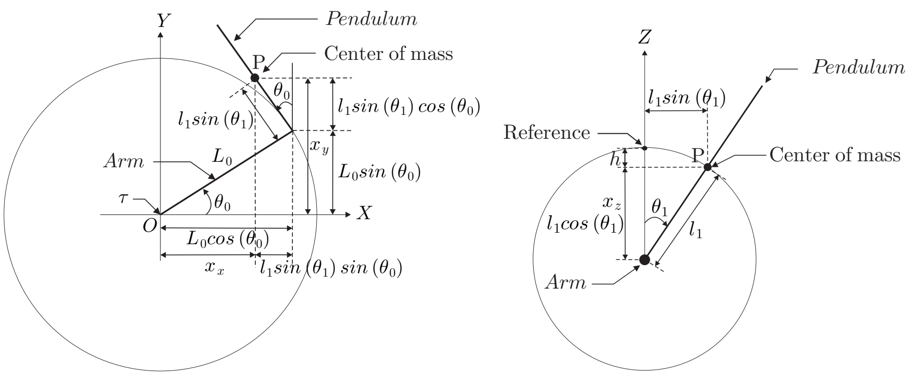

(a) Projection of the *arm* and *pendulum* in the horizontal plane.

(b) Projection of the *pendulum* in the vertical plane.

Fig. 2. Free body diagram of the system.

After replacing (7) in (5) and reducing the resulting expression, the following is found:

$$K_1 = \frac{1}{2} J_1 \dot{\theta}_1^2 + \frac{1}{2} m_1 \left[\left(\dot{\theta}_0 L_0 \right)^2 + \left(l_1 \dot{\theta}_0 sin\left(\theta_1\right) \right)^2 + \left(l_1 \dot{\theta}_1 \right)^2 + 2\dot{\theta}_0 \dot{\theta}_1 L_0 l_1 cos\left(\theta_1\right) \right].$$

Therefore, the Furuta pendulum kinetic energy K is given by

$$\begin{aligned} K &= K_0 + K_1, \\ &= \frac{1}{2} I_0 \dot{\theta}_0^2 + \frac{1}{2} J_1 \dot{\theta}_1^2 + \frac{1}{2} m_1 \left[\left(\dot{\theta}_0 L_0 \right)^2 + \left(l_1 \dot{\theta}_0 sin\left(\theta_1\right) \right)^2 + \left(l_1 \dot{\theta}_1 \right)^2 + \right. \\ &\quad \left. + \, 2\dot{\theta}_0 \dot{\theta}_1 L_0 l_1 cos\left(\theta_1\right) \right]. \end{aligned} \tag{8}$$

On the other hand, V is the sum of the potential energy of the *arm* and *pendulum*. Since the *arm* is moved on the horizontal plane, its potential energy is constant and can be considered equal to zero. Hence, the Furuta pendulum potential energy V is reduced to the *pendulum* potential energy, that is:

$$V = -h m_1 g = m_1 g l_1 \left(cos\left(\theta_1\right) - 1 \right). \tag{9}$$

Then, from (3), which has associated to (8) and (9), and after carrying out the corresponding derivatives in the equations system (1), (2), the dynamics of the Furuta pendulum is found as follows:

$$\alpha \ddot{\theta}_0 + \beta \dot{\theta}_0 \dot{\theta}_1 + \gamma \ddot{\theta}_1 - \sigma \dot{\theta}_1^2 = \tau, \tag{10}$$

$$\gamma \ddot{\theta}_0 + (m_1 l_1^2 + J_1) \ddot{\theta}_1 - \frac{1}{2} \beta \dot{\theta}_0^2 - m_1 g l_1 sin\left(\theta_1\right) = 0, \tag{11}$$

where $\ddot{\theta}_0$ is the *arm* angular acceleration, $\ddot{\theta}_1$ is the *pendulum* angular acceleration,

$$\begin{aligned} \alpha &= I_0 + m_1 L_0^2 + m_1 l_1^2 sin^2\left(\theta_1\right), & \gamma &= m_1 L_0 l_1 cos\left(\theta_1\right), \\ \beta &= m_1 l_1^2 sin(2\theta_1), & \sigma &= m_1 L_0 l_1 sin\left(\theta_1\right). \end{aligned}$$

3 Computer aided design and construction

The elements that integrate the Furuta pendulum test-bed and the procedure followed in the construction of such a test-bed are presented below.

As shown in Figure 3, the Furuta pendulum test-bed is composed –in general– of three blocks, namely: *subsystems*, *power stage*, and *data acquisition and processing*. The block *subsystems* refers to two subsystems, the first one corresponds to a DC permanent magnet motor and two encoders; whereas, the second corresponds to a mechanical structure, which includes the mechanical elements that are, directly and indirectly, moved by the DC motor and those that hold the system. The block *power stage* is integrated by two power electronic devices, which as a whole provide energy to the DC motor. The block *data acquisition and processing* is associated with Matlab-Simulink, ControlDesk, and a DS1104 board from dSPACE, which allow the acquisition and processing of the data provided by the encoders.

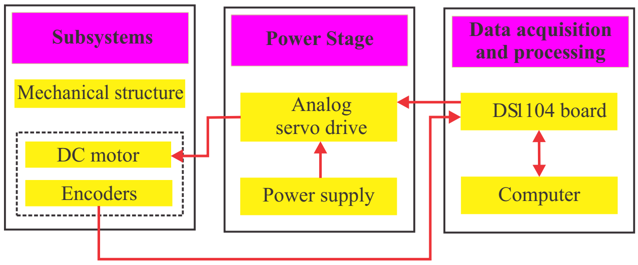

Fig. 3. Block diagram of the test-bed.

3.1 Subsystems

This Section describes the DC motor, encoders, and mechanical structure. The DC motor provides angular movement to the *arm*, the encoders are employed to sense the angular position of the *arm* and the *pendulum*, and the mechanical structure was designed via the software SolidWorks, which is a tool for mechanical design in 3D.

DC motor and encoders. Know the mechanical and electric characteristics of the DC motor is not an easy task; therefore, numerical simulations of the Furuta pendulum mathematical model were performed with the intention of determining the required torque to move the *pendulum* around its upright position (see Section 4). These simulations showed that the required torque is 0.17 Nm. Thus, a 14204 Brush DC motor from Pittman was used.

Regarding the encoders, the encoder that allows sensing the *arm* position is included in the DC motor chassis and it has a 500 CPR resolution; whereas, the encoder associated with the *pendulum* is an ITD 01 A 4 Y 1 optical mini encoder fabricated by Baumer with 1024 CPR as maximum resolution. Both encoders are of the incremental type.

Mechanical structure. The mechanical elements that compose the Furuta pendulum test-bed were drawn and assembled, virtually, by using SolidWorks, since this software includes advanced functions that facilitate the part modeling, create assemblies, and generate plans easily and quickly. Also, SolidWorks allows specifying the material properties for each part of the Furuta pendulum test-bed. Thus, a computer aided design of such a test-bed was generated as shown in Figure 4(a).

According to Figure 4(a), the description of each part that integrates the mechanical structure is as follows:

① The *Arm* was manufactured from a T–6061 T–6 aluminum round bar with a 5/8″ diameter.

② The *Pendulum* was made from a T–6061 aluminum tube with a 3/8″ outer diameter and a T–6061 aluminum sheet. Furthermore, the *pendulum* includes the shaft that must be mounted into the *pendulum* encoder. The shaft was manufactured from a C–1018 round AISI with a 1/2″ diameter.

③ This part corresponds to the DC motor with encoder described in Section 3.1.

④ This part is associated with the *pendulum* encoder described in Section 3.1.

⑤ The encoder holder is used to hold the encoder of the *pendulum*. This holder was made from a T–6061 aluminum sheet. This part includes a 628/6–2z deep groove ball bearing from SKF.

⑥ The upper sheet is used to hold the DC motor with encoder and was manufactured from a stainless steel sheet.

⑦ The vertical aluminum profiles were made from Bosch tubular profiles. The weight of the remaining parts that compose the mechanical structure rests on such vertical profiles.

⑧ The horizontal aluminum profiles keep apart the vertical profiles to a certain distance, providing structural stability to the test-bed.

⑨ The bottom sheet, manufactured from a stainless steel sheet, is used to hold the power supply that provides energy to the electrical and electronic devices.

⑩ The leveling legs are used to even the mechanical structure on a surface, which allows avoiding undesired movements of the test-bed.

The test-bed built can be seen in Figure 4(b).

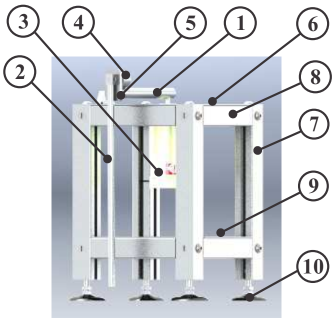

(a) Computer aided design of the test-bed.

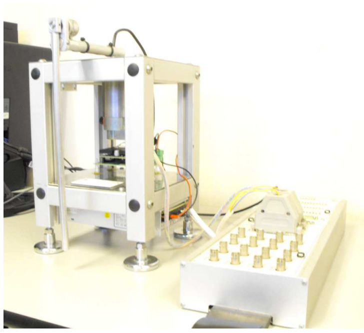

(b) Real test-bed connected to the DS1104 board.

Fig. 4. Furuta pendulum test-bed.

It is important to mention that the design of the Furuta pendulum test-bed was carried out in such a way that another configuration of pendulum can be set (see [14]).

3.2 Power Stage

As was mentioned previously, the block *Power Stage* consists of two power electronic devices. The first one refers to a switched power supply of the HF100W–SF–24 model. This power supply provides energy to the DC motor, by means of the second power electronic device, that is, an analog servo drive, which is used to isolate the block *data acquisition and processing* from the DC motor. Also, this servo drive amplifies the current of a signal provided by the *data acquisition and processing* block, being the amplified signal the DC motor input signal. The servo drive is fabricated by Advanced Motion Controls in the model AZ12A8DDC. An important characteristic of such a servo drive is that it includes an internal control-loop, which avoids losses when the amplified signal is delivered to the DC motor.

3.3 Data acquisition and processing

This Section describes the connection between the test-bed and the DS1104 board from dSPACE. This board was selected due to the integration software between Matlab-Simulink and ControlDesk, that is, the board firmware.

In order to connect the test-bed with the DS1104 board, a block diagram is programmed in the Matlab-Simulink environment. Such a program contains the blocks to generate the signal that has to be amplified by the analog servo drive. Also, the program includes the blocks related to the ports of the DS1104 board where the incremental encoders and the analog servo drive are connected. Latter, the program is executed by means of ControlDesk, which allows the acquisition and processing of the data provided by the encoders and by the DC motor input signal.

4 Simulations and experimental results

Numerical simulations associated with the model (10)-(11) and experiments obtained by using the test-bed built of the Furuta pendulum are presented below.

4.1 Results

In the implementation of the numerical simulations of the dynamics of the Furuta pendulum, that is, (10)-(11), the following values of the parameters were used:

$$\begin{aligned}&I_0 = 0.4592 \text{ x } 10^{-3} \text{ Kgm}^2, \quad l_1 = 0.1475 \text{ m}, \quad L_0 = 0.1414 \text{ m},\\ &J_1 = 0.2755 \text{ x } 10^{-3} \text{ Kgm}^2, \quad m_1 = 0.038 \text{ Kg}.\end{aligned}$$

Such values were obtained directly from the test-bed built. The numerical simulations consisted in apply a constant torque to the *arm* during a period of time equal to 0.2 s, moving it from an arbitrary position, achieving that the *pendulum* reaches a position between ± 1 rad around the upright position from its natural equilibrium point, that is, $\pm\pi$ rad. As regards to the experimental tests similar conditions to those used in the simulations were considered. Both simulations and experimental tests were carried out in open-loop. The numerical simulations were performed by using Matlab-Simulink and the experimental tests were carried out via Matlab-Simulink, ControlDesk, and a DS1104 board.

The simulation results are shown in Figure 5, also this figure includes the experimental results obtained from the test-bed built. With the purpose of differentiating the simulation results from the experimental ones, the following nomenclature was used. For the simulation results the variables θ_0 and θ_1 are denoted as θ_{0s} and θ_{1s}, respectively. Likewise, θ_{0e} and θ_{1e} denote the experimental results of the variables aforementioned. Whereas, the input of the system, τ, is denoted as τ_s for the case of the simulations and for the experimental results is defined as τ_e.

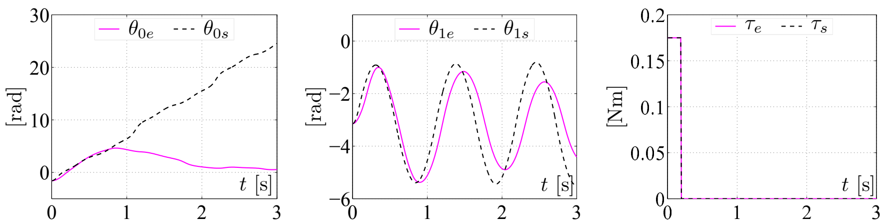

Fig. 5. Simulations and experimental results.

4.2 Discussion

The differences found when comparing the simulation and experimental results are mainly due to the friction forces, which are not considered in the deduction of the mathematical model (10)-(11). Also, another factor that limits the angular movement of the *arm* in real time experiments, that is θ_{0e}, is the cable of the encoder that senses the variable θ_1, temporarily placed in such a way that offers a minimum resistance to the *arm* movement.

5 Conclusion

This paper has introduced step-by-step the modeling, computer aided design, and construction of a Furuta pendulum test-bed. Also, experimental tests on the test-bed built were carried out with success, since the obtained results are in accordance with the ones obtained from numerical simulations of the Furuta pendulum mathematical model. The aforementioned has the propose of facilitating the modeling and construction of a Furuta pendulum test-bed, which can be used to experimentally validate automatic control strategies and study some features of nonlinear systems.

Regarding the future work, in the deduction of the Furuta pendulum mathematical model, consider the dynamics of the actuator and driver would be interesting. Some works associated with the dynamics of actuators and drivers are [15–18].

Acknowledgments

The work of Mayra Antonio-Cruz, Carlos Alejandro Merlo-Zapata, and Celso Márquez-Sánchez was supported by CONACYT-México and BEIFI scholarships. R. Silva-Ortigoza acknowledges financial support from Secretaría de Investigación y Posgrado del Instituto Politécnico Nacional (SIP-IPN), SNI-México, and the IPN programs EDI and COFAA. Likewise, Victor Manuel Hernández-Guzmán thanks financial support from SNI-México. Finally, Jacobo Sandoval-Gutiérrez acknowledges the financial support from Cátedras CONACYT-México and CIDETEC-IPN.

References

1. S. Jadlovská and J. Sarnovský, "Modelling of classical and rotary inverted pendulum systems–a generalized approach," *Journal of Electrical Engineering*, vol. 64, no. 1, pp. 12–19, 2013.
2. F. J. Muñoz-Almaraz, E. Freire, and J. Galán-Vioque, "Bifurcation behavior of the Furuta pendulum," *International Journal of Bifurcation and Chaos*, vol. 17, no. 8, pp. 2571–2578, 2007.
3. P. X. La Hera, L. B. Freidovich, A. S. Shiriaev, and U. Mettin, "New approach for swinging up the Furuta pendulum: Theory and experiments," *Mechatronics*, vol. 19, no. 8, pp. 1240–1250, 2009.
4. J. Sandoval, R. Kelly, and V. Santibáñez, "Interconnection and damping assignment passivity-based control of a class of underactuated mechanical systems with dynamic friction," *International Journal of Robust and Nonlinear Control*, vol. 21, no. 7, pp. 738–751, 2011.
5. P. Seman, B. Rohal'-Ilkiv, M. Juhás, and M. Salaj, "Swinging up the Furuta pendulum and its stabilization via model predictive control," *Journal of Electrical Engineering*, vol. 64, no. 3, pp. 152–158, 2013.
6. J. Aracil, J. Á. Acosta, and F. Gordillo, "A nonlinear hybrid controller for swinging-up and stabilizing the Furuta pendulum," *Control Engineering Practice*, vol. 21, no. 8, pp. 989–993, 2013.
7. M. Demirtas, Y. Altun, and A. Istanbullu, "Virtual laboratory for sliding mode and PID control of rotary inverted pendulum," *Computer Applications in Engineering Education*, vol. 21, no. 3, pp. 400–409, 2013.
8. V. M. Hernández-Guzmán, R. Silva-Ortigoza y R. V. Carrillo-Serrano, *Control Automático: Teoría de Diseño, Construcción de Prototipos, Modelado, Identificación y Pruebas Experimentales*, Colección CIDETEC–IPN, México, DF, México, 2013. [Online]. Available: http://www.controlautomatico.com.mx

9. J. Á. Acosta, "Furuta's pendulum: A conservative nonlinear model for theory validation and practise," *Mathematical Problems in Engineering*, vol. 2010, Article ID 742894, 29 pages, 2010.
10. B. S. Cazzolato and Z. Prime, "On the dynamics of the Furuta pendulum," *Journal of Control Science and Engineering*, vol. 2011, Article ID 528341, 8 pages.
11. B. Allota, L. Pugi, and F. Bartolini, "Reinforcement neural network for the stabilization of a Furuta pendulum," in *Proc. 2nd European Conference on Mechanism Science* (*EUCOMES*), Cassino, Italy, Sep. 17–20, 2008, pp. 287–294.
12. O. García-Alarcón, S, Puga-Guzmán, and J. Moreno-Valenzuela, "On parameter identification of the Furuta pendulum," in *Proc. International Meeting of Electrical Engineering Research* (*ENIINVIE*), Ensenada, B. C., Mexico, Mar. 28–30, 2012, pp. 77–84.
13. M. Antonio-Cruz, R. Silva-Ortigoza, C. A. Merlo-Zapata, M. G. Villarreal-Cervantes, D. Muñoz-Carrillo, and V. M. Hernández-Guzmán, "Modeling and construction of a Furuta pendulum prototype," *IEEE 2014 International Conference on Mechatronics, Electronics and Automotive Engineering* (*ICMEAE*), Morelos, Mexico, Nov. 2014. Article in Press.
14. C. A. Merlo-Zapata, M. Antonio-Cruz, R. Silva-Ortigoza, H. Taud, I. Rivera-Zárate, D. Muñoz-Carrillo, and V. M. Hernández-Guzmán, "Modeling and construction of an inertia wheel pendulum test-bed," *IEEE 2014 International Conference on Mechatronics, Electronics and Automotive Engineering* (*ICMEAE*), Morelos, Mexico, Nov. 2014. Article in Press.
15. R. Silva-Ortigoza, J. R. García-Sánchez, J. M. Alba-Martínez, V. M. Hernández-Guzmán, M. Marcelino-Aranda, H. Taud, and R. Bautista-Quintero, "Two-stage control design of a Buck converter/DC motor system without velocity measurements via a $\Sigma - \Delta$-modulator," *Mathematical Problems in Engineering*, vol. 2013, Article ID 929316, 11 pages, 2013. [Online]. Available at `http://dx.doi.org/10.1155/2013/929316`
16. R. Silva-Ortigoza, C. Márquez-Sánchez, F. Carrizosa-Corral, M. Antonio-Cruz, J. M. Alba-Martínez, and G. Saldaña-González "Hierarchical velocity control based on differential flatness for a DC/DC Buck converter–DC motor system," *Mathematical Problems in Engineering*, vol. 2014, Article ID 912815, 12 pages, 2014. [Online]. Available at `http://dx.doi.org/10.1155/2014/912815`
17. R. Silva-Ortigoza, V. M. Hernández-Guzmán, M. Antonio-Cruz, and D. Muñoz-Carrillo, "DC/DC Buck power converter as a smooth starter for a DC motor based on a hierarchical control," *IEEE Transactions on Power Electronics*, vol. 30, no. 2, pp. 1076–1084, 2015. [Online]. Available with DOI: `10.1109/TPEL.2014.2311821`
18. V. M. Hernández-Guzmán, R. Silva-Ortigoza, and D. Muñoz-Carrillo, "Velocity control of a brushed dc-motor driven by a DC to DC Buck power converter," *International Journal of Innovative Computing, Information and Control*, vol. 11, no. 2, 13 pages, 2015.